The Influence of Temperature on Ozone Production under varying NO_x Conditions – a modelling study

J. Coates[1], K. A. Mar[1], N. Ojha[2], and T. M. Butler[1]

[1]Institute for Advanced Sustainability Studies, Potsdam, Germany
[2]Atmospheric Chemistry Department, Max Planck Institute for Chemistry, Mainz, Germany

Correspondence to: J. Coates (jane.coates@iass-potsdam.de)

Abstract. Surface ozone is a secondary air pollutant produced during the atmospheric photochemical degradation of emitted volatile organic compounds (VOCs) in the presence of sunlight and nitrogen oxides (NO_x). Temperature directly influences ozone production through speeding up the rates of chemical reactions and increasing the emissions of VOCs, such as isoprene, from vegetation. In this study, we used a box model to examine the non-linear relationship between ozone, NO_x and temperature, and compared this to previous observational studies. Under high-NO_x conditions, an increase in ozone from 20 °C to 40 °C of up to 20 ppbv was due to faster reaction rates while increased isoprene emissions added up to a further 11 ppbv of ozone. The increased oxidation rate of emitted VOC with temperature controlled the rate of O_x production, the net influence of peroxy nitrates increased net O_x production per molecule of emitted VOC oxidised. The rate of increase in ozone mixing ratios with temperature from our box model simulations was about half the rate of increase in ozone with temperature observed over central Europe or simulated by a regional chemistry transport model. Modifying the box model setup to approximate stagnant meteorological conditions increased the rate of increase of ozone with temperature as the accumulation of oxidants enhanced ozone production through the increased production of peroxy radicals from the secondary degradation of emitted VOCs. The box model simulations approximating stagnant conditions and the maximal ozone production chemical regime reproduced the 2 ppbv increase in ozone per °C from the observational and regional model data over central Europe. The simulated ozone-temperature relationship was more sensitive to mixing than the choice of chemical mechanism. Our analysis suggests that reductions in NO_x emissions would be required to offset the additional ozone production due to an increase in temperature in the future.

1 Introduction

Surface-level ozone (O_3) is a secondary air pollutant formed during the photochemical degradation of volatile organic compounds (VOCs) in the presence of nitrogen oxides ($NO_x \equiv NO + NO_2$). Due to the photochemical nature of ozone production, it is strongly influenced by meteorological variables such as temperature (Jacob and Winner, 2009). In particular, heatwaves, characterised by high temperatures and stagnant meteorological conditions, are correlated with high ozone levels as was the case during the European heatwave in 2003 (Solberg et al., 2008; Vautard et al., 2005). Furthermore, Otero et al. (2016) showed that temperature was a major meteorological driver of summertime ozone concentrations in many areas of central Europe.

Temperature primarily influences ozone production in two ways: speeding up the rates of many chemical reactions, and increasing emissions of VOCs from biogenic sources (BVOCs) (Sillman and Samson, 1995). While emissions of anthropogenic VOCs (AVOCs) are generally not dependent on temperature, evaporative emissions of some AVOCs do increase with temperature (Rubin et al., 2006). The review of Pusede et al. (2015) provides further details of the temperature-dependent processes impacting ozone production.

Regional modelling studies over the US (Sillman and Samson, 1995; Steiner et al., 2006; Dawson et al., 2007) examined the sensitivity of ozone production during a pollution episode to increased temperatures. These studies noted that increased temperatures (without changing VOC or NO_x-conditions) led to higher ozone levels, often exceeding local air quality guidelines. Sillman and Samson (1995) and Dawson et al. (2007) varied the temperature dependence of the PAN (peroxy acetyl nitrate) decomposition rate during simulations of the eastern US determining the sensitivity of ozone production with temperature to the PAN decomposition rate. In addition to the influence of PAN decomposition on ozone production, Steiner et al. (2006) correlated the increase in ozone mixing ratios with temperature over California to increased mixing ratios of formaldehyde, a secondary degradation production of many VOCs and an important radical source. Steiner et al. (2006) also noted increased emissions of BVOCs at higher temperatures in urban areas with high NO_x emissions also increased ozone levels with temperature.

The modelling study of Vogel et al. (1999) looked at the NO_y transition value as an indicator of ozone sensitivity at different VOC and NO_x conditions and investigated how this transition value changed with different meteorological conditions. Higher temperatures led to a higher transition value of NO_y which was attributed to the faster thermal decomposition of PAN. Vogel et al. (1999) also showed vertical mixing and dry deposition decreased the transition value of NO_y showing that ozone production is sensitive to other non-chemical processes.

Pusede et al. (2014) used an analytical model constrained by observations over the San Joaquin Valley, California to infer a non-linear relationship between ozone, temperature and NO_x, similar to the well-known non-linear relationship of ozone production on NO_x and VOC levels (Sillman, 1999). Moreover, Pusede et al. (2014) showed that temperature can be used as a surrogate for VOC levels when considering the relationship of ozone under different NO_x conditions.

Environmental chamber studies have also been used to analyse the relationship of ozone with temperature using a fixed mixture of VOCs. The chamber experiments of Carter et al. (1979) and Hatakeyama et al. (1991) showed increases in ozone from a VOC mix with temperature. Both studies compared the concentration time series of ozone and nitrogen-containing compounds (NO_x, PAN, HNO_3) at various temperatures linking the maximum ozone concentration to the decrease in PAN concentrations at temperatures greater than 303 K.

The review of Pusede et al. (2015) highlights a general lack of modelling studies looking at the relationship of ozone with temperature under different NO_x conditions. The regional modelling studies described previously concentrated on reproducing ozone levels (using a single chemical mechanism) over regions with known meteorology and NO_x conditions then varying the temperature. These regional modelling studies did not consider the relationship between ozone, NO_x and temperature. Vogel et al. (1999) only considered the effect of faster reaction rates at higher temperature and not the additional contribution of increased biogenic emissions to ozone levels at higher temperatures.

Comparisons of different chemical mechanisms, such as Emmerson and Evans (2009) and Coates and Butler (2015), showed that different representations of tropospheric chemistry influenced ozone production. Neither of these studies examined the ozone-temperature relationship differences between chemical mechanisms. Furthermore, Rasmussen et al. (2013) acknowledged that the modelled ozone-temperature relationship may be sensitive to the choice of chemical mechanism and recommended investigating this sensitivity. Comparing the ozone-temperature relationship predicted by different chemical mechanisms is potentially important for modelling of future air quality due to the expected increase in heatwaves (Karl and Trenberth, 2003).

In this study, we use an idealised box model to determine how ozone levels vary with temperature under different NO_x conditions. We determine whether faster chemical reaction rates or increased BVOC emissions have a greater influence on instantaneous ozone production with higher temperature under different NO_x conditions. Furthermore, we compare the ozone-temperature relationship produced by different chemical mechanisms and determine which chemical processes drive the increase of ozone with temperature. We compare the rate of increase of ozone with temperature obtained from the box model to both observations and regional model ouput and consider the role of stagnation on the rate of increase of ozone with temperature.

2 Methodology

2.1 Model Setup

We performed idealised simulations using the MECCA box model (Sander et al., 2005) to determine the important gas-phase chemical processes for ozone production under different temperatures and NO_x conditions. The MECCA box model was set up as described in Coates and Butler (2015) and updated to include vertical mixing with the free troposphere using a diurnal cycle for the PBL height. The vertical mixing scheme was based on the approach of Lourens et al. (2016) with the model using the mean mixing layer height from the BAERLIN campaign over Berlin, Germany (Bonn et al., 2016).

Simulations were run for daylight hours in one full day using a latitude of 51 °N, broadly representative of conditions in central Europe. Methane was fixed at 1.7 ppmv throughout the model run, carbon monoxide (CO) and ozone were initialised at 200 ppbv and 40 ppbv and then allowed to evolve freely throughout the simulation. All VOC emissions were held constant until noon simulating a plume of freshly-emitted VOC. the mixing ratios of O_3, CO and CH_4 in the free troposphere were respectively set to 50 ppbv, 116 ppbv and 1.8 ppmv. These conditions were taken from the MATCH-MPIC chemical weather forecast model on the 21st March (the start date of the simulations). The model results (http://cwf.iass-potsdam.de/) at the 700 hPa height were chosen and the daily average was used as input into the boxmodel.

Separate box model simulations were performed by systematically varying the temperature between 288 and 313 K (15–40 °C) in steps of 0.5 K. NO emissions were systematically varied between 5.0×10^9 and 1.5×10^{12} molecules(NO) cm^{-2} s^{-1} in steps of 1×10^{10} molecules(NO) cm^{-2} s^{-1} at each temperature step. At 20 °C, these NO emissions corresponded to peak NO_x mixing ratios of 0.02 ppbv and 10 ppbv respectively, this range of NO_x mixing ratios covers the NO_x conditions found in pristine and urban conditions (von Schneidemesser et al., 2015).

All simulations were repeated using different chemical mechanisms to investigate whether the relationship between ozone, temperature and NO_x changes using different representations of ozone production chemistry. The reference chemical mechanism was the near-explicit Master Chemical Mechanism, MCMv3.2, (Jenkin et al., 1997, 2003; Saunders et al., 2003; Rickard et al., 2015). The reduced chemical mechanisms in our study were Common Representative Intermediates, CRIv2 (Jenkin et al., 2008), Model for OZone and Related Chemical Tracers, MOZART-4 (Emmons et al., 2010), Regional Acid Deposition Model, RADM2 (Stockwell et al., 1990) and the Carbon Bond Mechanism, CB05 (Yarwood et al., 2005). These reduced chemical mechanisms were chosen as they are all currently used by modelling groups in 3D regional and global models (Baklanov et al., 2014). Coates and Butler (2015) described the implementation of these chemical mechanisms in MECCA.

The chemical mechanisms use temperature-dependent rate constants, k(T), to represent temperature-dependent chemical processes, including the initial oxidation of VOC, peroxy nitrate (RO_2NO_2) formation and destruction, and reactions between peroxy radicals and NO leading to alkyl nitrate ($RONO_2$) formation. However, not all chemical mechanisms represent the same chemical processes by a temperature-dependent rate constant. For example, in CB05, the rate constant of $RONO_2$ formation during isoprene degradation is temperature dependent while $RONO_2$ formation during alkane degradation is temperature independent. Furthermore, none of the chemical mechanisms in our study represent the $RONO_2$ branching ratio as a temperature dependent process. Experiments have shown the temperature dependence of the $RONO_2$ branching ratio for some VOCs (Atkinson et al., 1987) but generally $RONO_2$ chemistry is not well known (Pusede et al., 2015).

Model runs were repeated using a temperature-independent and temperature-dependent source of BVOC emissions to determine the relative importance of increased emissions of BVOC and faster reaction rates of chemical processes for the increase of ozone with temperature. Many types of VOCs are emitted from vegetation with isoprene and monoterpenes globally having the largest emissions, 535 and 162 Tg yr^{-1} respectively (Guenther et al., 2012). Temperature-dependent emissions of these highly-reactive BVOC in urban areas during the summer months have been linked to high levels of ozone pollution. For example, Wang et al. (2013) attributed high summertime levels of ozone in Taipei to increased isoprene emissions from vegetation during the hotter summer months. Vegetation in urban areas also provides additional ozone sinks through stomatal uptake and ozonolysis of emitted BVOCs, the review of Calfapietra et al. (2013) discusses the role of BVOCs emitted by trees in urban areas in more detail.

Biogenic emissions of monoterpenes and isoprene are included in all model simulations. Model runs using a temperature-dependent source of BVOC emissions considered only the temperature-dependence of isoprene emissions as specified by MEGAN2.1 (Guenther et al., 2012), Sect. 2.3 provides further details. Since isoprene is the most important BVOC on the global scale, we focused on the influence of the temperature-dependence of isoprene emissions on ozone levels. Future work should assess the influence of temperature-dependent biogenic emissions of monoterpenes on ozone production. In the temperature-dependent set of model simulations, only isoprene emissions were dependent on temperature and all other emissions were constant in all simulations. In reality, evaporative emissions from anthropogenic sources increase with temperature (Rubin et al., 2006) and isoprene has also been measured from vehicular exhausts (Borbon et al., 2001). Representing a temperature-dependent evaporative source of AVOC and an anthropogenic source of isoprene requires detailed local knowledge of these emission sources. Since our box modelling study was designed as an idealised study and not characterise the influence of

all temperature-dependent emission sources in a particular region, we have not considered the potential larger increase of ozone at higher temperatures due to these additional emission sources. Further modelling work assessing the influence of these temperature-dependent emission sources on ozone production would be useful for mitigating ozone pollution in urban areas.

2.2 VOC Emissions

Emissions of urban AVOC over central Europe were taken from the TNO-MACC_III emission inventory for the Benelux (Belgium, Netherlands and Luxembourg) region for the year 2011. TNO-MACC_III is the updated TNO-MACC_II emission inventory created using the same methodology as Kuenen et al. (2014) and based upon improvements to the existing emission inventory during AQMEII-2 (Pouliot et al., 2015).

Temperature-independent emissions of isoprene and monoterpenes from biogenic sources were calculated as a fraction of the total AVOC emissions from each country in the Benelux region. This data was obtained from the supplementary data available from the EMEP (European Monitoring and Evaluation Programme) model (Simpson et al., 2012). Temperature-dependent emissions of isoprene are described in Sect. 2.3.

Table 1 shows the quantity of VOC emissions from each source category and the temperature-independent BVOC emissions. These AVOC emissions were assigned to chemical species and groups based on the profiles provided by TNO. The NMVOC emissions were speciated to MCMv3.2 species as described by von Schneidemesser et al. (2016). For simulations done with other chemical mechanisms, the VOC emissions represented by the MCMv3.2 were mapped to the mechanism species representing VOC emissions in each reduced chemical mechanism based on the recommendations of the source literature and Carter (2015). The VOC emissions in the reduced chemical mechanisms were weighted by the carbon numbers of the MCMv3.2 species and the emitted mechanism species, thus keeping the amount of emitted reactive carbon constant between simulations. The supplementary data outlines the primary VOC and calculated emissions with each chemical mechanism.

2.3 Temperature Dependent Isoprene Emissions

Temperature-dependent emissions of isoprene were estimated using the MEGAN2.1 algorithm for calculating the emissions of VOC from vegetation (Guenther et al., 2012). Emissions from nature are dependent on many variables including temperature, radiation and age of vegetation but for the purpose of our study all variables except temperature were held constant. To directly compare the effects of temperature-dependent emissions of isoprene to temperature-dependent chemistry, the MEGAN2.1 parameters used to calculate isoprene emissions online by the model were chosen to give similar isoprene mixing ratios at 20 °C to the temperature-independent emissions of isoprene. The estimated emissions of isoprene with MEGAN2.1 using these assumptions are illustrated in Fig. 1 and show the expected exponential increase in isoprene emissions with temperature (Guenther et al., 2006).

The estimated emissions of isoprene at 20 °C lead to 0.07 ppbv of isoprene in our simulations while at 30 °C, the increased emissions of isoprene using MEGAN2.1 estimations lead to 0.35 ppbv of isoprene in the model. A measurement campaign over Essen, Germany (Wagner and Kuttler, 2014) measured 0.1 ppbv of isoprene at temperature 20 °C and 0.3 ppbv of isoprene were measured at 30 °C. The similarity of the simulated and observed isoprene mixing ratios indicates that the MEGAN2.1

variables chosen for calculating the temperature-dependent emissions of isoprene were suitable for simulating urban conditions over central Europe.

3 Results and Discussion

3.1 Relationship between Ozone, NO_x and Temperature

Figure 2 depicts the peak mixing ratio of ozone from each simulation as a function of the total NO_x emissions and temperature when using a temperature-independent and temperature-dependent source of isoprene emissions for each chemical mechanism. The relative difference in ozone mixing ratio produced using each reduced chemical mechanism from the MCMv3.2 is shown in A non-linear relationship of ozone mixing ratios with NO_x and temperature is produced by each chemical mechanism. This non-linear relationship is similar to that determined by Pusede et al. (2014) using an analytical model constrained to observational measurements over the San Joaquin Valley, California.

Higher peak ozone mixing ratios are produced when using a temperature-dependent source of isoprene emissions (Fig. 2). The highest mixing ratios of peak ozone are produced at high temperatures and moderate emissions of NO_x regardless of the temperature dependence of isoprene emissions. Conversely, the least amount of peak ozone is produced with low emissions of NO_x over the whole temperature range (15 – 40 °C) when using both a temperature-independent and temperature-dependent source of isoprene emissions. The larger increases in ozone levels in the Maximal-O3 and High-NO_x regimes indicate that strong reductions in NO_x emissions are neccessary to offset the increase in ozone pollution at higher temperatures when isoprene emissions are higher.

The contours of ozone mixing ratios as a function of NO_x and temperature can be split into three NO_x regimes (Low-NO_x, Maximal-O_3 and High-NO_x), similar to the NO_x regimes defined for the non-linear relationship of ozone with VOC and NO_x. The Low-NO_x regime corresponds with regions having little increase in ozone with temperature, also called the NO_x-sensitive regime. The High-NO_x (or NO_x-saturated) regime is when ozone levels increase rapidly with temperature. The contour ridges correspond to regions of maximal ozone production; this is the Maximal-O_3 regime. Pusede et al. (2014) showed that temperature can be used as a proxy for VOC, thus we assigned the ozone mixing ratios from each box model simulation to a NO_x regime based on the H_2O_2:HNO_3 ratio. This ratio was used by Sillman (1995) and Staffelbach et al. (1997) to designate ozone to NO_x regimes based on NO_x and VOC levels. The Low-NO_x regime corresponds to H_2O_2:HNO_3 ratios less than 0.5, the High-NO_x regime corresponds to ratios larger than 0.3 and ratios between 0.3 and 0.5 correspond to the Maximal-O_3 regime.

The peak ozone mixing ratio from each simulation was assigned to a NO_x regime based on the H_2O_2:HNO_3 ratio of that simulation. The peak ozone mixing ratios assigned to each NO_x regime at each temperature were averaged, and illustrated in Fig. 3 for each chemical mechanism and each type of isoprene emissions (temperature independent and temperature dependent). We define the absolute increase in ozone from 20 °C to 40 °C due to faster reaction rates as the difference between ozone mixing ratios from 20 °C to 40 °C when using a temperature-independent source of isoprene emissions. When using a temperature-dependent source of isoprene emissions, the difference in ozone mixing ratios from 20 °C to 40 °C minus the increase due to

faster reaction rates, gives the absolute increase in ozone mixing ratios from increased isoprene emissions. These differences are represented graphically in Fig. 3 and summarised in Table 2.

Table 2 shows that the absolute increase in ozone with temperature due to chemistry (i.e. faster reaction rates) is larger than the absolute increase in ozone due to increased isoprene emissions for each chemical mechanism and each NO_x regime. In all cases the absolute increase in ozone with temperature is largest under High-NO_x conditions and lowest with Low-NO_x conditions (Fig. 3 and Table 2). The increase in ozone mixing ratio from 20 °C to 40 °C due to faster reaction rates with High-NO_x conditions is almost double that with Low-NO_x conditions. In the Low-NO_x regime, the increase of ozone with temperature using the reduced chemical mechanisms (CRIv2, MOZART-4, CB05 and RADM2) is similar to that from the MCMv3.2. Larger differences occur in the Maximal-O_3 and High-NO_x regimes.

All reduced chemical mechanisms except RADM2 have similar increases in ozone due to increased isoprene emissions as the MCMv3.2 (Table 2). RADM2 produces 3 ppbv less ozone than the MCMv3.2 due to increased isoprene emissions in each NO_x regime, indicating that this difference is due the representation of isoprene degradation chemistry in RADM2.

Coates and Butler (2015) compared ozone production in different chemical mechanisms to the MCMv3.2 using the TOPP metric (Tagged Ozone Production Potential) as defined in Butler et al. (2011) and showed that less ozone is produced per molecule of isoprene emitted using RADM2 than with MCMv3.2. The degradation of isoprene has been extensively studied and it is well-known that methyl vinyl ketone (MVK) and methacrolein are signatures of isoprene degradation (Atkinson, 2000). All chemical mechanisms in our study except RADM2 explicitly represent MVK and methacrolein (or in the case of CB05, a lumped species representing both these secondary degradation products). RADM2 does not represent methacrolein and the mechanism species representing ketones (KET) is a mixture of acetone and methyl ethyl ketone (MEK) (Stockwell et al., 1990). Thus the secondary degradation of isoprene in RADM2 is unable to represent the ozone production from the further degradation of the signature secondary degradation products of isoprene, MVK and methacrolein. Updated versions of RADM2, RACM (Stockwell et al., 1997) and RACM2 (Goliff et al., 2013), sequentially included methacrolein and MVK and with these updates the ozone production from isoprene oxidation approached that of the MCMv3.2 (Coates and Butler, 2015).

Regions of high temperatures and high NO_x emissions in leave to the largest inter-mechanism differences between ozone mixing ratios using reduced chemical mechanisms from the MCMv3.2 (up to XXX ppbv). The maximum difference between ozone mixing ratios produced using the chemical mechanisms (at 40 °C) in the High-NO_x state (Fig. 3) is 10 ppbv when using both a temperature-independent and temperature-dependent source of isoprene emissions. These differences in ozone mixing ratios between the chemical mechanisms are similar to that obtained by Coates and Butler (2015) (8 ppbv) and von Schneidemesser et al. (2016) (7 ppbv).

The Maximal-O3 regime is reached with $\sim$ 30 % more NO_x emissions using CB05 and RADM2 than the MCMv3.2 at each temperature for both a temperature-independent and temperature-dependent source of isoprene emissions. The CRIv2 and MOZART-4 chemical mechanisms require very similar NO_x emissions to the MCMv3.2 at each temperature to produce maximum levels of ozone. Thus when modelling the air quality over a particular region using RADM2 and CB05, these mechanisms would predict a faster increase of ozone with temperature (i.e. more VOC-sensitive ozone production). This is consistent with the results of Fig. 3 and the slope of the rate of increase of ozone with temperature ($m_{O3\text{-}T}$) in Table 3. The

study using the 3D WRF-Chem model of Mar et al. (2016) compared ozone levels produced using MOZART-4 and RADM2 and also noted that RADM2 is in a more VOC-sensitive state than MOZART-4. These differences in the ozone production regime using different chemical mechanisms highlights the need for air quality studies to assess the chemical scheme used by the model.

Our simulations produced a non-linear relationship between ozone, temperature and NO_x with the absolute increase in ozone with temperature due to temperature-dependent chemistry larger than the increase in ozone with temperature due to temperature-dependent isoprene emissions. These results are consistent between each chemical mechanism, although RADM2 and CB05 simulate a more VOC-sensitive regime for the same temperature range than the other chemical mechanisms (MCMv3.2, CRIv2, MOZART-4). In order to determine the chemical processes responsible for the increased ozone with temperature, we analyse the production and consumption budgets of ozone in Sect. 3.2.

3.2 Ozone Production and Consumption Budgets

Since chemical reactions contributing to both production and consumption of O_x ($\equiv O_3 + NO_2 + O(^1D) + O$) have temperature-dependent rate constants, we analysed the production and consumption budgets of O_x to consider the effects of temperature-dependent reaction rates on ozone production. The O_x budgets displayed in Fig. 4 are assigned to each NO_x regime for each chemical mechanism and source of isoprene emissions. The net production or consumption of O_x is also displayed in Fig. 4.

Figure 4 was obtained by determining the chemical reactions producing and consuming O_x and then allocating these reactions to important categories. Reactions of peroxy radicals with NO produce O_x and the peroxy radicals are divided into 'HO2', 'RO2', 'ARO2' representing the reactions of NO with HO_2, alkyl peroxy radicals and acyl peroxy radicals respectively. Thus at each time step the O_x production rate is given by

$$k_{HO_2+NO}[HO_2][NO] + \sum_i k_{RO_{2,i}+NO}[RO_{2,i}][NO] + \sum_j k_{ARO_{2,j}+NO}[ARO_{2,j}][NO] \quad (1)$$

for each alkyl peroxy radical i and acyl peroxy radical j. The net contributions of peroxy nitrates, inorganic reactions and any other remaining organic reactions on the O_x budget are represented by the 'RO2NO2', 'Inorganic' and 'Other Organic' categories in Fig. 4b. The net contributions of these categories to the O_x budget was calculated by subtracting the consumption rate from the production rate of the reactions contributing to each category. For example, RO_2NO_2 produce O_x when thermally decomposing or reacting with OH and consume O_x when produced by RO_2 reacting with NO_2. Hence, at each time step the net contribution of RO2NO2 to the O_x budget was calculated by

$$\sum_k k_{RO_2NO_{2,k}}[RO_2NO_{2,k}] + \sum_k k_{RO_2NO_{2,k}+OH}[RO_2NO_{2,k}][OH] - \sum_k k_{RO_{2,k}+NO_2}[RO_{2,k}][NO_2] \quad (2)$$

for each peroxy nitrate species k. The cumulative day-time budgets were calculated by summing the net contributions of the reaction rates of each category over the day-time period. The ratio of net ozone to net O_x production was practically constant with temperature in all cases showing that using O_x budgets as a proxy for ozone budgets was suitable at each temperature in our study.

The absolute production and consumption budgets allocated to the major categories are displayed in Fig. 4a. Both production and consumption O_x budgets increase with temperature for each chemical mechanism and each NO_x conditions. The overall net increase of O_x production with temperature (white line in Fig. 4a) is consistent with the increase in ozone mixing ratios for each panel in Fig. 3. Moreover, the net chemical production of O_x is larger when using a temperature-dependent source of isoprene emissions than a temperature-independent source of isoprene emissions, again this is consistent with Fig. 3.

In order to determine which temperature-dependent chemical processes are responsible for the overall increase of net O_x production with temperature, the absolute O_x budgets in Fig. 4a were normalised by the total chemical loss rate of the emitted VOC (Fig. 4b). Thus Fig. 4b gives a measure of the O_x production and consumption efficiency per chemical loss of VOC. The net O_x production efficiency (white line in Fig. 4b) increases from 20 °C to 40 °C by ~ 0.25 molecules of O_x per molecule of VOC oxidised with each NO_x-condition and type of isoprene emissions using the detailed MCMv3.2 chemical mechanism. A lower increase in normalised net O_x production efficiency from 20 °C to 40 °C was obtained with the reduced chemical mechanisms (~ 0.2 molecules of O_x per molecule of VOC oxidised with CRIv2, CB05 and RADM2, and ~ 0.1 molecules of O_x per molecule of VOC oxidised using MOZART-4). The increase in net O_x production efficiency is due to the increased contribution with temperature of acyl peroxy radicals (ARO2) reacting with NO and the decreased net contribution with temperature of RO2NO2 (peroxy nitrates) to the normalised O_x budgets.

The increased contribution of ARO2 to O_x production with temperature is linked to the decreased net contribution of RO2NO2 with temperature to O_x budgets as peroxy nitrates are produced from the reactions of acyl peroxy radicals with $NO2$. The decomposition rate of peroxy nitrates is strongly temperature dependent and at higher temperatures the faster decomposition rate of RO_2NO_2 leads to faster release of acyl peroxy radicals and NO_2. Thus the equilibrium of RO_2NO_2 shifts towards thermal decomposition with increasing temperature leading to the increased contribution of ARO2 with temperature to O_x production (Fig. 4b). Dawson et al. (2007) attributed the increase in maximum 8 h ozone mixing ratios with temperature during a modelling study over the eastern US to the decrease in PAN lifetime with temperature. Steiner et al. (2006) also recognised that the decrease in PAN lifetime with temperature contributed to the increase of ozone with temperature concluding that the combined effects of increased oxidation rates of VOC and faster PAN decomposition increased the production of ozone with temperature.

As the production efficiency of O_x remains constant with temperature (~ 2 molecules of O_x per molecule of VOC oxidised, Fig. 4b), the rate of O_x production is controlled by the oxidation rate of VOCs. Faster oxidation of VOCs with temperature speeds up the production of peroxy radicals increasing ozone production when peroxy radicals react with NO to produce NO_2. The reactivity of VOCs has been linked to ozone production (e.g. Kleinman (2005), Sadanaga et al. (2005)) and the review of Pusede et al. (2015) acknowledged the importance of organic reactivity and radical production to the ozone-temperature relationship. Also, the modelling study of Steiner et al. (2006) noted that the increase in initial oxidation rates of VOCs with temperature leads to increased formaldehyde concentrations and in turn an increase of ozone as formaldehyde is an important source of HO_2 radicals.

Our results indicate that increased VOC reactivity and decomposition rate of peroxy nitrates are the temperature-dependent chemical processes leading to increased O_x with temperature. These results are consistent between each chemical mechanism

and each NO_x condition. Of the emitted VOC, reactive VOCs such as alkenes and aromatics were responsible for the increased VOC oxidation with temperature. The study of Li et al. (2014) also showed that reactive VOC such as ethene and xylene were responsible for ozone formation in Asia. Over longer timescales, the contribution of less-reactive VOC, such as alkanes, may also significantly contribute to ozone production (Butler et al., 2011; von Schneidemesser et al., 2016).

3.3 Comparison to Observations and 3D Model Simulations

The final step in our study was to compare our idealised simulations to real-world observations, we wanted to see how our idealised setup could simulate the real-world relationship between ozone and temperature. Using the interpolated observations of the maximum daily 8 h mean (MDA8) of ozone from Schnell et al. (2015) and the meteorological observational data set of the ERA-Interim re-analysis, Otero et al. (2016) showed that over the summer (JJA) months, temperature is the main meteorological driver of ozone production over many regions of central Europe. A further test was to include the output from a regional 3D model, 3D models are setup to simulate areas to investigate air quality over specific regions and include many more real-world processes (horizontal transport, stratospheric influence, changing meteorological parameters such as humidity, wind speed among others) that are not included in our box model setup. Model output from the 3D WRF-Chem regional model using MOZART-4 chemistry set-up over the European domain for simulations of the year 2007 from Mar et al. (2016) was used to further compare the box model simulations to a model including more meteorological processes than our box model.

Our idealised box model was setup to investigate the reasons for the observed increase of ozone with temperature and a direct comparison of the ozone mixing ratios produced from the simulations are thus difficult to directly compare side-by-side to both the observations and WRF-Chem output. In particular, the ozone mixing ratios reported by observations and simulated using WRF-Chem are a function of more processes than included in our box model. For example, VOCs are constantly emitted, NO_x emissions have a diurnal profile, more realistic meterology processes such as the influence of low wind speed (when combined with warm temperatures give rise to stagnant conditions) whereas in the box model, VOC emissions are emitted as a 6 hour pulse, NO emissions are held constant and besides vertical mixing into a clean troposphere, there are no other transport processes. Moreover, there are further differences between the box model and WRF-Chem such as how photolysis is treated and particle-phase chemistry is also utilised within WRF-Chem whereas our box model only considered gas-phase chemistry. Despite these differences, it is interesting to compare the rate of change of ozone with temperature ($m_{O3\text{-}T}$) between the box model, observations and the more realistic WRF-Chem model. This metric has been used by many studies (Sillman and Samson, 1995; Baertsch-Ritter et al., 2004; Rasmussen et al., 2013) and is calculated taking the linear slope of the increase of ozone with temperature. Table 3 summarises the slopes ($m_{O3\text{-}T}$) of the linear fits of the box model simulations displayed in Fig. 5 in ppbv of ozone per °C determining the rate of increase of ozone with temperature.

Figure 5 compares the observational and WRF-Chem data from summer 2007 averaged over central and eastern Germany, where summertime ozone values are driven by temperature (Otero et al., 2016), to the MDA8 values of ozone from the box model simulations for each chemical mechanism (solid lines). The observational data produces an increase of 2.15 ppbv/°C which is comparable to that of 2.2 ppbv/°C obtained for the Northeast US after NO_x reductions from power plants (Rasmussen et al., 2013) as well as that reported by Sillman and Samson (1995) for the average rural US (2.4 ppbv/°C) and Milan, Italy

(2.8 ppbv/°C, Baertsch-Ritter et al. (2004)). Despite a high bias in simulated ozone in WRF-Chem, the rate of change of ozone with temperature from the WRF-Chem simulations (2.05 ppbv/°C) is similar to the rate of change of ozone with temperature from the observed data (2.15 ppbv/°C). The differences in ozone production between the different chemical mechanisms with the box model are small compared to the spread of the observational and WRF-Chem data. A temperature-dependent source of isoprene with high-NO_x conditions produces the highest ozone-temperature slope, but is still lower than the observed ozone-temperature slope by a factor of two. In particular, the box model simulations over-predict the ozone values at lower temperatures and under-predict the ozone values at higher temperatures compared to the observed data.

As mentioned earlier, there are number of differences between our box model setup and both the observational and 3D model output and of these differences the one most relevant to our study could be the lack of stagnation. Stagnant atmospheric conditions are characteristed by low wind speeds slowing the transport of ozone and its precursors away from sources and have been correlated to high-ozone episodes in the summer over eastern US (Jacob et al., 1993). In order to investigate the sensitivity of ozone production to mixing, box model simulations were performed without vertical mixing to approximate stagnant conditions that favour accumulation of secondary VOC oxidation products. The ozone-temperature relationship obtained with each chemical mechanism, using both a temperature-independent and temperature-dependent source of isoprene emissions and the different NO_x conditions are displayed in Fig. 5 (dotted lines).

For all chemical mechanisms, the rate of increase of ozone with temperature increased in the box model simulations without mixing. The $m_{O3\text{-}T}$ calculated from the box model simulations without mixing using a temperature-dependent source of isoprene and with Maximal-O_3 conditions (ranging between 2.0 and 2.4 ppbv/°C) are very similar to the slopes of the observational and WRF-Chem results (2.1 and 2.2 ppbv/°C, respectively). The differences in $m_{O3\text{-}T}$ when not including mixing in the box model compared to the differences in $m_{O3\text{-}T}$ between chemical mechanisms in Table 3 show that the ozone-temperature relationship using our box model setup is more sensitive to mixing than the choice of chemical mechanism.

An analysis similar to that presented in Fig. 4b shows no appreciable difference between the cases with and without mixing (not shown). The chemical production of O_x in each chemical mechanism normalised by the chemical loss rate of VOC remains unchanged. Furthermore, the supplementary material includes the absolute production and consumption budgets of O_x which also show the increased O_x production with temperature for the simulations performed without mixing. From this we conclude that the increased ozone production seen in the box model simulations with reduced mixing is due to enhanced OH reactivity from secondary VOC oxidation products.

Thus our box model study does not reproduce the rate of increase of ozone with temperature obtained from observational and 3D model simulations. The reason for this discrepancy was that the box model did not represent stagnation conditions which are relevant to real-world conditions and in particular for simulating heatwaves. The lack of mixing meant that the main chemical processes leading to ozone levels with increased temperature discussed in Sect. 3.2, namely increase oxidation of VOC and faster peroxy nitrate thermal decomposition, were able to proceed without the chemical reactants being transported away from the region. This is particular important for times of heatwaves, indicating that stronger reductions in NO_x and possibly VOCs during heatwaves are required to minimise the impact of increase ozone production at higher temperatures.

4 Conclusions

In this study, we determined the effects of temperature on ozone production using a box model over a range of temperatures and NO_x conditions with a temperature-independent and temperature-dependent source of isoprene emissions. These simulations were repeated using reduced chemical mechanism schemes (CRIv2, MOZART-4, CB05 and RADM2) typically used in 3D models and compared to the near-explicit MCMv3.2 chemical mechanism.

Each chemical mechanism produced a non-linear relationship of ozone with temperature and NO_x with the most ozone produced at high temperatures and moderate emissions of NO_x. Conversely, lower NO_x levels led to a minimal increase of ozone with temperature. Thus air quality in a future with higher temperatures would benefit from reductions in NO_x emissions.

Faster reaction rates at higher temperatures were responsible for a greater absolute increase in ozone than increased isoprene emissions. In our simulations, ozone production was controlled by the increased rate of VOC oxidation with temperature. The net influence of peroxy nitrates increased the net production of O_x per molecule of emitted VOC oxidised with temperature.

The rate of increase of ozone with temperature using observational data over Europe was twice as high as the rate of increase of ozone with temperature when using the box model. This was consistent with our box model setup not representing stagnant atmospheric conditions that are inherently included in observational data and models including meteorology, such as WRF-Chem. In model simulations without mixing the rate of increase of ozone with temperature was faster than the simulations including mixing. The simulations without mixing and a maximal ozone production chemical regime led to very similar rates of increase of ozone with temperature to the observational and WRF-Chem data. Furthermore, the ozone-temperature relationship was more sensitive to mixing than the choice of chemical mechanism.

Author contributions. T. M. Butler and J. Coates designed the experiment, J. Coates performed box model simulations and analysis. K. A. Mar and N. Ojha performed WRF-Chem model runs and provided this data. J. Coates prepared the manuscript with comments from all co-authors.

Acknowledgements. The authors would like to thank Noelia Otero Felipe for providing the ERA-Interim data.

References

Atkinson, R.: Atmospheric chemistry of VOCs and NO_x, Atmospheric Environment, 34, 2063–2101, 2000.

Atkinson, R., Aschmann, S. M., and Winer, A. M.: Alkyl nitrate formation from the reaction of a series of branched RO2 radicals with NO as a function of temperature and pressure, Journal of Atmospheric Chemistry, 5, 91–102, 1987.

Baertsch-Ritter, N., Keller, J., Dommen, J., and Prevot, A. S. H.: Effects of various meteorological conditions and spatial emissionresolutions on the ozone concentration and ROG/NO_x limitation in the Milan area (I), Atmospheric Chemistry and Physics, 4, 423–438, 2004.

Baklanov, A., Schlünzen, K., Suppan, P., Baldasano, J., Brunner, D., Aksoyoglu, S., Carmichael, G., Douros, J., Flemming, J., Forkel, R., Galmarini, S., Gauss, M., Grell, G., Hirtl, M., Joffre, S., Jorba, O., Kaas, E., Kaasik, M., Kallos, G., Kong, X., Korsholm, U., Kurganskiy, A., Kushta, J., Lohmann, U., Mahura, A., Manders-Groot, A., Maurizi, A., Moussiopoulos, N., Rao, S. T., Savage, N., Seigneur, C., Sokhi, R. S., Solazzo, E., Solomos, S., Sørensen, B., Tsegas, G., Vignati, E., Vogel, B., and Zhang, Y.: Online coupled regional meteorology chemistry models in Europe: current status and prospects, Atmospheric Chemistry and Physics, 14, 317–398, 2014.

Bonn, B., von Schneidemesser, E., Andrich, D., Quedenau, J., Gerwig, H., Lüdecke, A., Kura, J., Pietsch, A., Ehlers, C., Klemp, D., Kofahl, C., Nothard, R., Kerschbaumer, A., Junkermann, W., Grote, R., Pohl, T., Weber, K., Lode, B., Schönberger, P., Churkina, G., Butler, T. M., and Lawrence, M. G.: BAERLIN2014 – the influence of land surface types on and the horizontal heterogeneity of air pollutant levels in Berlin, Atmospheric Chemistry and Physics, 16, 7785–7811, 2016.

Borbon, A., Fontaine, H., Veillerot, M., Locoge, N., Galloo, J., and Guillermo, R.: An investigation into the traffic-related fraction of isoprene at an urban location, Atmospheric Environment, 35, 3749 – 3760, 2001.

Butler, T., Lawrence, M., Taraborrelli, D., and Lelieveld, J.: Multi-day ozone production potential of volatile organic compounds calculated with a tagging approach, Atmospheric Environment, 45, 4082 – 4090, 2011.

Calfapietra, C., Fares, S., Manes, F., Morani, A., Sgrigna, G., and Loreto, F.: Role of Biogenic Volatile Organic Compounds (BVOC) emitted by urban trees on ozone concentration in cities: A review, Environmental Pollution, 183, 71 – 80, 2013.

Carter, W. P. L.: Development of a Database for Chemical Mechanism Assignments for Volatile Organic Emissions, Journal of the Air & Waste Management Association, 0, 2015.

Carter, W. P. L., Winer, A. M., Darnall, K. R., and Jr., J. N. P.: Smog chamber studies of temperature effects in photochemical smog, Environmental Science & Technology, 13, 1094–1100, 1979.

Coates, J. and Butler, T. M.: A comparison of chemical mechanisms using tagged ozone production potential (TOPP) analysis, Atmospheric Chemistry and Physics, 15, 8795–8808, 2015.

Dawson, J. P., Adams, P. J., and Pandis, S. N.: Sensitivity of ozone to summertime climate in the eastern USA: A modeling case study , Atmospheric Environment, 41, 1494 – 1511, 2007.

Emmerson, K. M. and Evans, M. J.: Comparison of tropospheric gas-phase chemistry schemes for use within global models, Atmospheric Chemistry and Physics, 9, 1831–1845, 2009.

Emmons, L. K., Walters, S., Hess, P. G., Lamarque, J.-F., Pfister, G. G., Fillmore, D., Granier, C., Guenther, A., Kinnison, D., Laepple, T., Orlando, J., Tie, X., Tyndall, G., Wiedinmyer, C., Baughcum, S. L., and Kloster, S.: Description and evaluation of the Model for Ozone and Related chemical Tracers, version 4 (MOZART-4), Geoscientific Model Development, 3, 43–67, 2010.

Goliff, W. S., Stockwell, W. R., and Lawson, C. V.: The regional atmospheric chemistry mechanism, version 2, Atmospheric Environment, 68, 174 – 185, 2013.

Guenther, A., Karl, T., Harley, P., Wiedinmyer, C., Palmer, P. I., and Geron, C.: Estimates of global terrestrial isoprene emissions using MEGAN (Model of Emissions of Gases and Aerosols from Nature), Atmospheric Chemistry and Physics, 6, 3181–3210, 2006.

Guenther, A. B., Jiang, X., Heald, C. L., Sakulyanontvittaya, T., Duhl, T., Emmons, L. K., and Wang, X.: The Model of Emissions of Gases and Aerosols from Nature version 2.1 (MEGAN2.1): an extended and updated framework for modeling biogenic emissions, Geoscientific Model Development, 5, 1471–1492, 2012.

Hatakeyama, S., Akimoto, H., and Washida, N.: Effect of temperature on the formation of photochemical ozone in a propene-nitrogen oxide (NOx)-air-irradiation system, Environmental Science & Technology, 25, 1884–1890, 1991.

Jacob, D. J. and Winner, D. A.: Effect of climate change on air quality, Atmospheric Environment, 43, 51 – 63, 2009.

Jacob, D. J., Logan, J. A., Gardner, G. M., Yevich, R. M., Spivakovsky, C. M., Wofsy, S. C., Sillman, S., and Prather, M. J.: Factors regulating ozone over the United States and its export to the global atmosphere, Journal of Geophysical Research, 98, 1993.

Jenkin, M., Watson, L., Utembe, S., and Shallcross, D.: A Common Representative Intermediates (CRI) mechanism for VOC degradation. Part 1: Gas phase mechanism development, Atmospheric Environment, 42, 7185 – 7195, 2008.

Jenkin, M. E., Saunders, S. M., and Pilling, M. J.: The tropospheric degradation of volatile organic compounds: a protocol for mechanism development, Atmospheric Environment, 31, 81 – 104, 1997.

Jenkin, M. E., Saunders, S. M., Wagner, V., and Pilling, M. J.: Protocol for the development of the Master Chemical Mechanism, MCM v3 (Part B): tropospheric degradation of aromatic volatile organic compounds, Atmospheric Chemistry and Physics, 3, 181–193, 2003.

Karl, T. R. and Trenberth, K. E.: Modern Global Climate Change, Science, 302, 1719–1723, 2003.

Kleinman, L. I.: The dependence of tropospheric ozone production rate on ozone precursors, Atmospheric Environment, 39, 575 – 586, 2005.

Kuenen, J. J. P., Visschedijk, A. J. H., Jozwicka, M., and Denier van der Gon, H. A. C.: TNO-MACC_II emission inventory; a multi-year (2003–2009) consistent high-resolution European emission inventory for air quality modelling, Atmospheric Chemistry and Physics, 14, 10 963–10 976, 2014.

Li, M., Zhang, Q., Streets, D. G., He, K. B., Cheng, Y. F., Emmons, L. K., Huo, H., Kang, S. C., Lu, Z., Shao, M., Su, H., Yu, X., and Zhang, Y.: Mapping Asian anthropogenic emissions of non-methane volatile organic compounds to multiple chemical mechanisms, Atmospheric Chemistry and Physics, 14, 5617–5638, 2014.

Lourens, A. S. M., Butler, T. M., Beukes, J. P., van Zyl, P. G., Fourie, G. D., and Lawrence, M. G.: Investigating atmospheric photochemistry in the Johennesburg-Pretoria megacity using a box model, South African Journal of Science, 112, 2016.

Mar, K. A., Ojha, N., Pozzer, A., and Butler, T. M.: Ozone air quality simulations with WRF-Chem (v3.5.1) over Europe: Model evaluation and chemical mechanism comparison, Geoscientific Model Development Discussions, 2016, 1–50, 2016.

Otero, N., Sillmann, J., Schnell, J. L., Rust, H. W., and Butler, T.: Synoptic and meteorological drivers of extreme ozone concentrations over Europe, Environmental Research Letters, 11, 024 005, 2016.

Pouliot, G., van der Gon, H. A. D., Kuenen, J., Zhang, J., Moran, M. D., and Makar, P. A.: Analysis of the emission inventories and model-ready emission datasets of Europe and North America for phase 2 of the AQMEII project, Atmospheric Environment, 115, 345–360, 2015.

Pusede, S. E., Gentner, D. R., Wooldridge, P. J., Browne, E. C., Rollins, A. W., Min, K.-E., Russell, A. R., Thomas, J., Zhang, L., Brune, W. H., Henry, S. B., DiGangi, J. P., Keutsch, F. N., Harrold, S. A., Thornton, J. A., Beaver, M. R., St. Clair, J. M., Wennberg, P. O., Sanders, J., Ren, X., VandenBoer, T. C., Markovic, M. Z., Guha, A., Weber, R., Goldstein, A. H., and Cohen, R. C.: On the temperature dependence of organic reactivity, nitrogen oxides, ozone production, and the impact of emission controls in San Joaquin Valley, California, Atmospheric Chemistry and Physics, 14, 3373–3395, 2014.

Pusede, S. E., Steiner, A. L., and Cohen, R. C.: Temperature and Recent Trends in the Chemistry of Continental Surface Ozone, Chemical Reviews, 115, 3898–3918, 2015.

Rasmussen, D. J., Hu, J., Mahmud, A., and Kleeman, M. J.: The Ozone–Climate Penalty: Past, Present, and Future, Environmental Science & Technology, 47, 14 258–14 266, 2013.

Rickard, A., Young, J., Pilling, M. J., Jenkin, M. E., Pascoe, S., and Saunders, S. M.: The Master Chemical Mechanism Version MCM v3.2, http://mcm.leeds.ac.uk/MCMv3.2/, [Online; accessed 25-March-2015], 2015.

Rubin, J. I., Kean, A. J., Harley, R. A., Millet, D. B., and Goldstein, A. H.: Temperature dependence of volatile organic compound evaporative emissions from motor vehicles, Journal of Geophysical Research: Atmospheres, 111, d03305, 2006.

Sadanaga, Y., Yoshino, A., Kato, S., , and Kajii, Y.: Measurements of OH Reactivity and Photochemical Ozone Production in the Urban Atmosphere, Environmental Science & Technology, 39, 8847–8852, pMID: 16323785, 2005.

Sander, R., Kerkweg, A., Jöckel, P., and Lelieveld, J.: Technical note: The new comprehensive atmospheric chemistry module MECCA, Atmospheric Chemistry and Physics, 5, 445–450, 2005.

Saunders, S. M., Jenkin, M. E., Derwent, R. G., and Pilling, M. J.: Protocol for the development of the Master Chemical Mechanism, MCM v3 (Part A): tropospheric degradation of non-aromatic volatile organic compounds, Atmospheric Chemistry and Physics, 3, 161–180, 2003.

Schnell, J. L., Prather, M. J., Josse, B., Naik, V., Horowitz, L. W., Cameron-Smith, P., Bergmann, D., Zeng, G., Plummer, D. A., Sudo, K., Nagashima, T., Shindell, D. T., Faluvegi, G., and Strode, S. A.: Use of North American and European air quality networks to evaluate global chemistry–climate modeling of surface ozone, Atmospheric Chemistry and Physics, 15, 10 581–10 596, 2015.

Sillman, S.: The use of NOy, H2O2, and HNO3 as indicators for ozone-NOx-hydrocarbon sensitivity in urban locations, Journal of Geophysical Research: Atmospheres, 100, 14 175–14 188, 1995.

Sillman, S.: The relation between ozone, NOx and hydrocarbons in urban and polluted rural environments, Atmospheric Environment, 33, 1821 – 1845, 1999.

Sillman, S. and Samson, P. J.: Impact of temperature on oxidant photochemistry in urban, polluted rural and remote environments, Journal of Geophysical Research: Atmospheres, 100, 11 497–11 508, 1995.

Simpson, D., Benedictow, A., Berge, H., Bergström, R., Emberson, L. D., Fagerli, H., Flechard, C. R., Hayman, G. D., Gauss, M., Jonson, J. E., Jenkin, M. E., Nyíri, A., Richter, C., Semeena, V. S., Tsyro, S., Tuovinen, J.-P., Valdebenito, Á., and Wind, P.: The EMEP MSC-W chemical transport model – technical description, Atmospheric Chemistry and Physics, 12, 7825–7865, 2012.

Solberg, S., Hov, Ø., Søvde, A., Isaksen, I. S. A., Coddeville, P., De Backer, H., Forster, C., Orsolini, Y., and Uhse, K.: European surface ozone in the extreme summer 2003, Journal of Geophysical Research: Atmospheres, 113, D07307, 2008.

Staffelbach, T., Neftel, A., Blatter, A., Gut, A., Fahrni, M., Stähelin, J., Prévôt, A., Hering, A., Lehning, M., Neininger, B., Bäumle, M., Kok, G. L., Dommen, J., Hutterli, M., and Anklin, M.: Photochemical oxidant formation over southern Switzerland: 1. Results from summer 1994, Journal of Geophysical Research: Atmospheres, 102, 23 345–23 362, 1997.

Steiner, A. L., Tonse, S., Cohen, R. C., Goldstein, A. H., and Harley, R. A.: Influence of future climate and emissions on regional air quality in California, Journal of Geophysical Research: Atmospheres, 111, d18303, 2006.

Stockwell, W. R., Middleton, P., Chang, J. S., and Tang, X.: The second generation regional acid deposition model chemical mechanism for regional air quality modeling, Journal of Geophysical Research: Atmospheres, 95, 16 343–16 367, 1990.

Stockwell, W. R., Kirchner, F., Kuhn, M., and Seefeld, S.: A new mechanism for regional atmospheric chemistry modeling, Journal of Geophysical Research: Atmospheres, 102, 25 847–25 879, 1997.

Figure 1. The estimated isoprene emissions (molecules isoprene cm^{-2} s^{-1}) using MEGAN2.1 at each temperature used in the study.

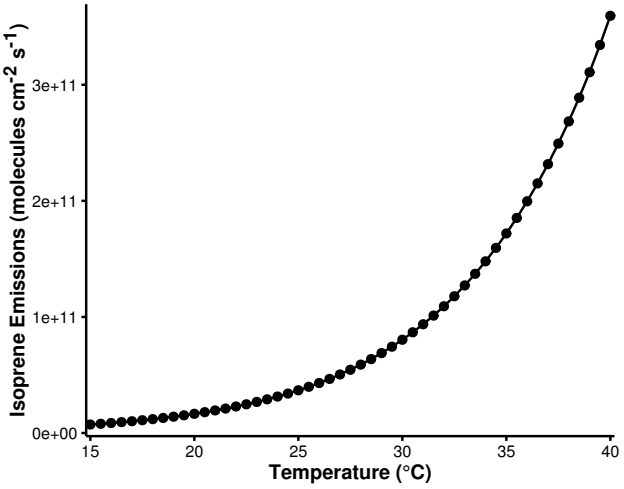

Vautard, R., Honoré, C., Beekmann, M., and Rouil, L.: Simulation of ozone during the August 2003 heat wave and emission control scenarios, Atmospheric Environment, 39, 2957 – 2967, 2005.

Vogel, B., Riemer, N., Vogel, H., and Fiedler, F.: Findings on NOy as an indicator for ozone sensitivity, Journal of Geophysical Research, 104, 3605–3620, 1999.

von Schneidemesser, E., Monks, P. S., Allan, J. D., Bruhwiler, L., Forster, P., Fowler, D., Lauer, A., Morgan, W. T., Paasonen, P., Righi, M., Sindelarova, K., and Sutton, M. A.: Chemistry and the Linkages between Air Quality and Climate Change, Chemical Reviews, pMID: 25926133, 2015.

von Schneidemesser, E., Coates, J., Visschedijk, A. J. H., Denier van der Gon, H. A. C., and Butler, T. M.: Variation of the NMVOC speciation in the solvent sector and the sensitivity of modelled tropospheric ozone, Atmospheric Environment, Submitted for Publication, 2016.

Wagner, P. and Kuttler, W.: Biogenic and anthropogenic isoprene in the near-surface urban atmosphere — A case study in Essen, Germany, Science of The Total Environment, 475, 104 – 115, 2014.

Wang, J., Chew, C., Chang, C.-Y., Liao, W.-C., Lung, S.-C. C., Chen, W.-N., Lee, P.-J., Lin, P.-H., and Chang, C.-C.: Biogenic isoprene in subtropical urban settings and implications for air quality, Atmospheric Environment, 79, 369–379, 2013.

Yarwood, G., Rao, S., Yocke, M., and Whitten, G. Z.: Updates to the Carbon Bond Chemical Mechanism: CB05, Tech. rep., U. S Environmental Protection Agency, 2005.

Table 1. Total AVOC emissions in 2011 in tonnes from each anthropogenic source category assigned from TNO-MACC_III emission inventory and temperature-independent BVOC emissions in tonnes from Benelux region assigned from EMEP. The allocation of these emissions to MCMv3.2, CRIv2, CB05, MOZART-4 and RADM2 species are found in the supplementary material.

Source Category	**Total Emissions**	**Source Category**	**Total Emissions**
Public Power	13755	Road Transport: Diesel	6727
Residential Combustion	21251	Road Transport: Others	1433
Industry	62648	Road Transport: Evaporation	2327
Fossil Fuel	15542	Non-road Transport	17158
Solvent Use	100826	Waste	1342
Road Transport: Gasoline	24921	BVOC	10702

Table 2. Increase in mean ozone mixing ratio (ppbv) due to chemistry (i.e. faster reaction rates) and temperature-dependent isoprene emissions from 20 °C to 40 °C in the NO_x-regimes of Fig. 3.

Chemical	**Source of**	**Increase in Ozone from 20 °C to 40 °C (ppbv)**		
Mechanism	**Difference**	**Low-NO_x**	**Maximal-O_3**	**High-NO_x**
MCMv3.2	Isoprene Emissions	4.6	7.7	10.6
	Chemistry	6.8	12.5	15.2
CRIv2	Isoprene Emissions	4.8	7.9	10.8
	Chemistry	6.0	11.1	13.7
MOZART-4	Isoprene Emissions	4.1	6.7	10.0
	Chemistry	6.0	10.2	12.3
CB05	Isoprene Emissions	4.6	7.4	9.8
	Chemistry	9.3	16.0	19.9
RADM2	Isoprene Emissions	3.8	5.7	7.8
	Chemistry	8.6	14.1	17.3

Figure 2. Contours of peak ozone mixing ratios (ppbv) as a function of the total NO_x emissions and temperature for each chemical mechanism using a temperature-dependent and temperature-independent source of isoprene emissions. The contours can be split into three separate regimes: High-NO_x, Maximal-O_3 and Low-NO_x indicated in the figure.

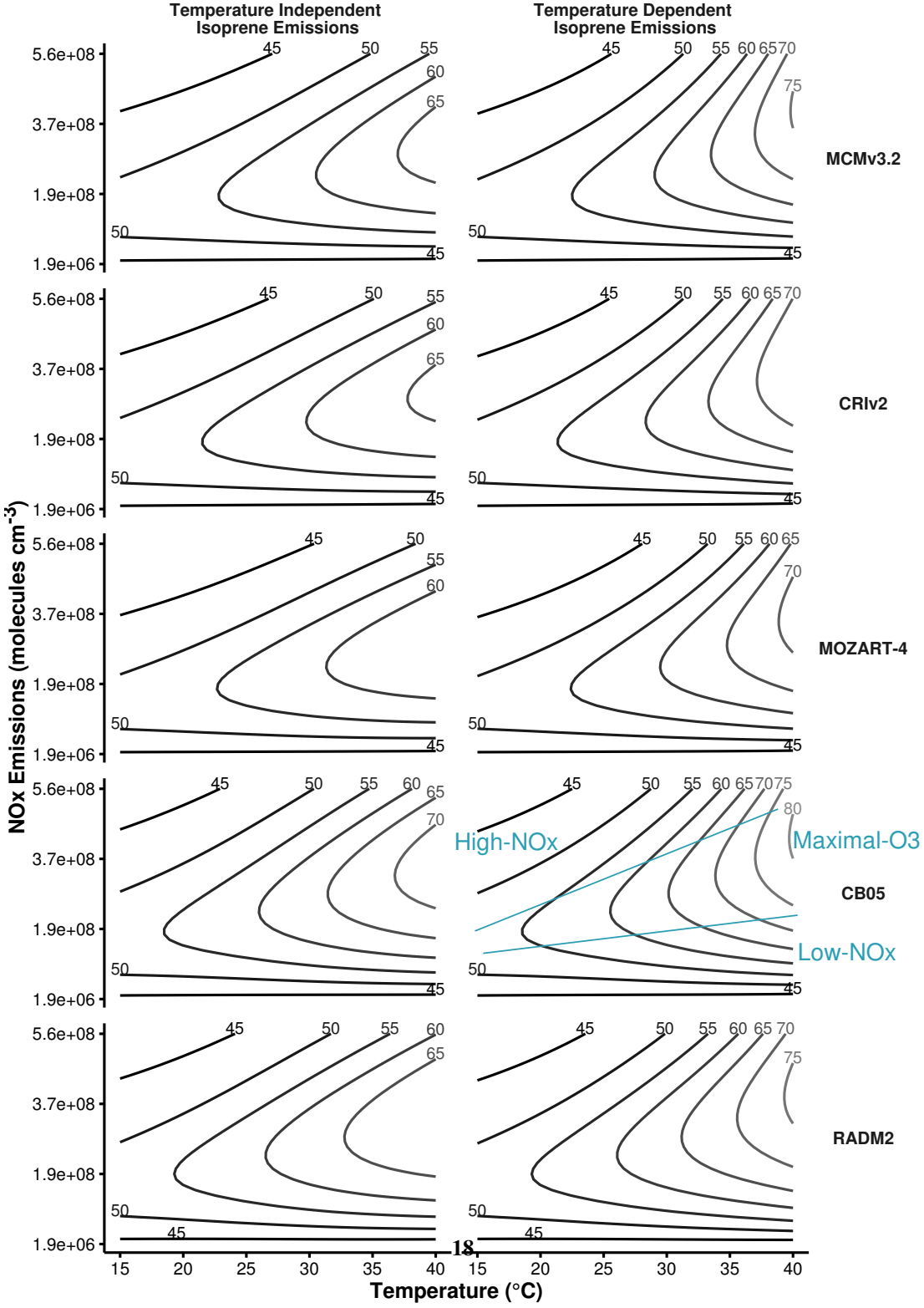

Figure 3. Mean ozone mixing ratios (ppbv) at each temperature after allocation to the different NO_x-regimes of Fig. 2. The differences in ozone mixing ratios due to chemistry (solid line) and isoprene emissions (dotted line) are represented graphically for MOZART-4 with High-NO_x conditions. Table 2 details the differences for each chemical mechanism and NO_x-condition.

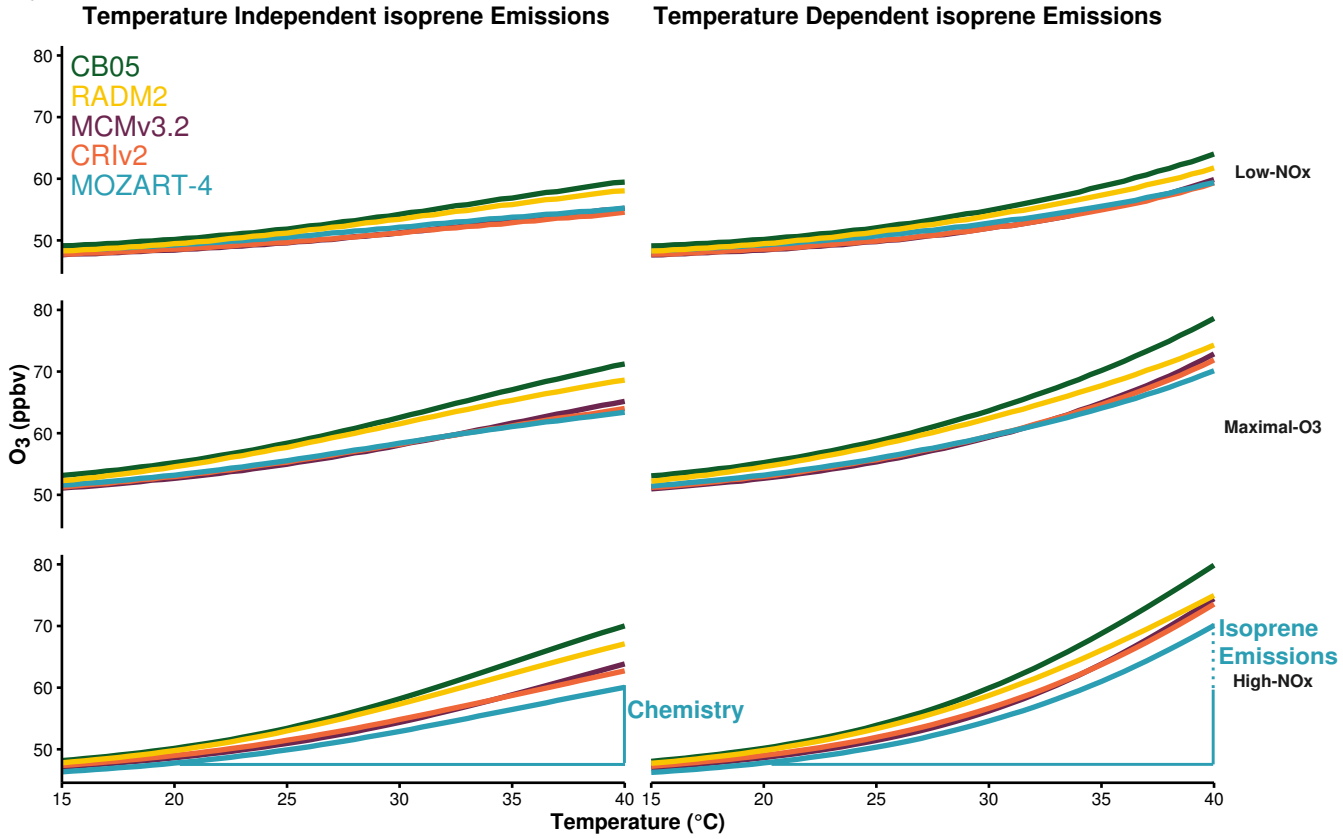

Figure 4. Day-time production and consumption budgets of O_x in the NO_x-regimes. The white line indicates net production or consumption of O_x. The net contribution of reactions to O_x budgets are allocated to categories of inorganic reactions, peroxy nitrates (RO2NO2), reactions of NO with HO2, alkyl peroxy radicals (RO2) and acyl peroxy radicals (ARO2). All other reactions are allocated to the 'Other Organic' category.

(a) O_x production and consumption budgets.

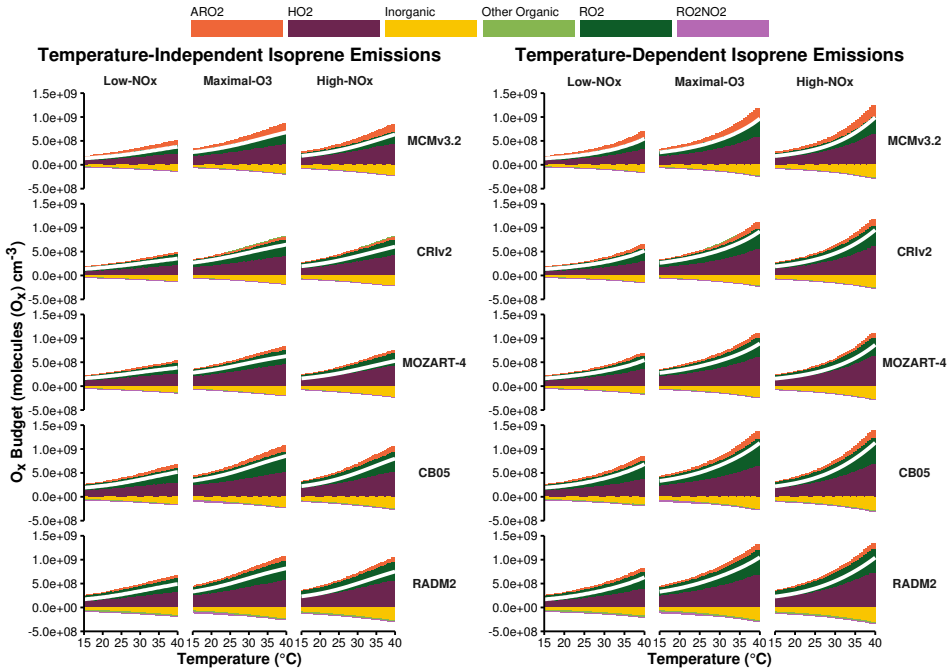

(b) O_x production and consumption budgets normalised by the total loss rate of emitted VOC.

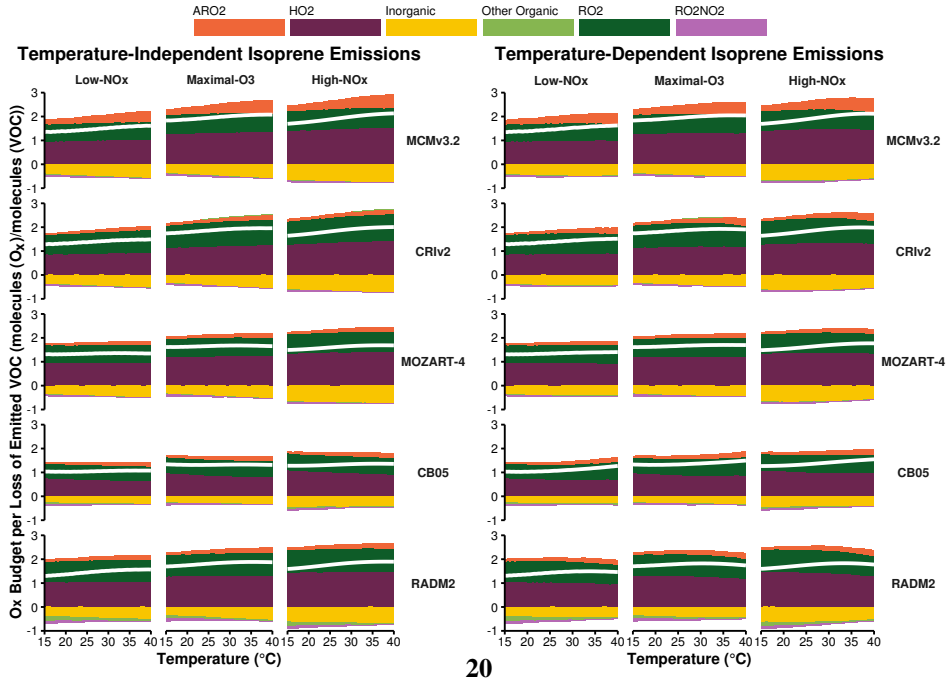

Figure 5. MDA8 values of ozone from the box model simulations allocated to the different NO_x regimes for each chemical mechanism with mixing (solid lines) and without mixing (dashed lines). The box model ozone-temperature correlation is compared to the summer 2007 observational data (black circles) and WRF-Chem output (purple boxes).

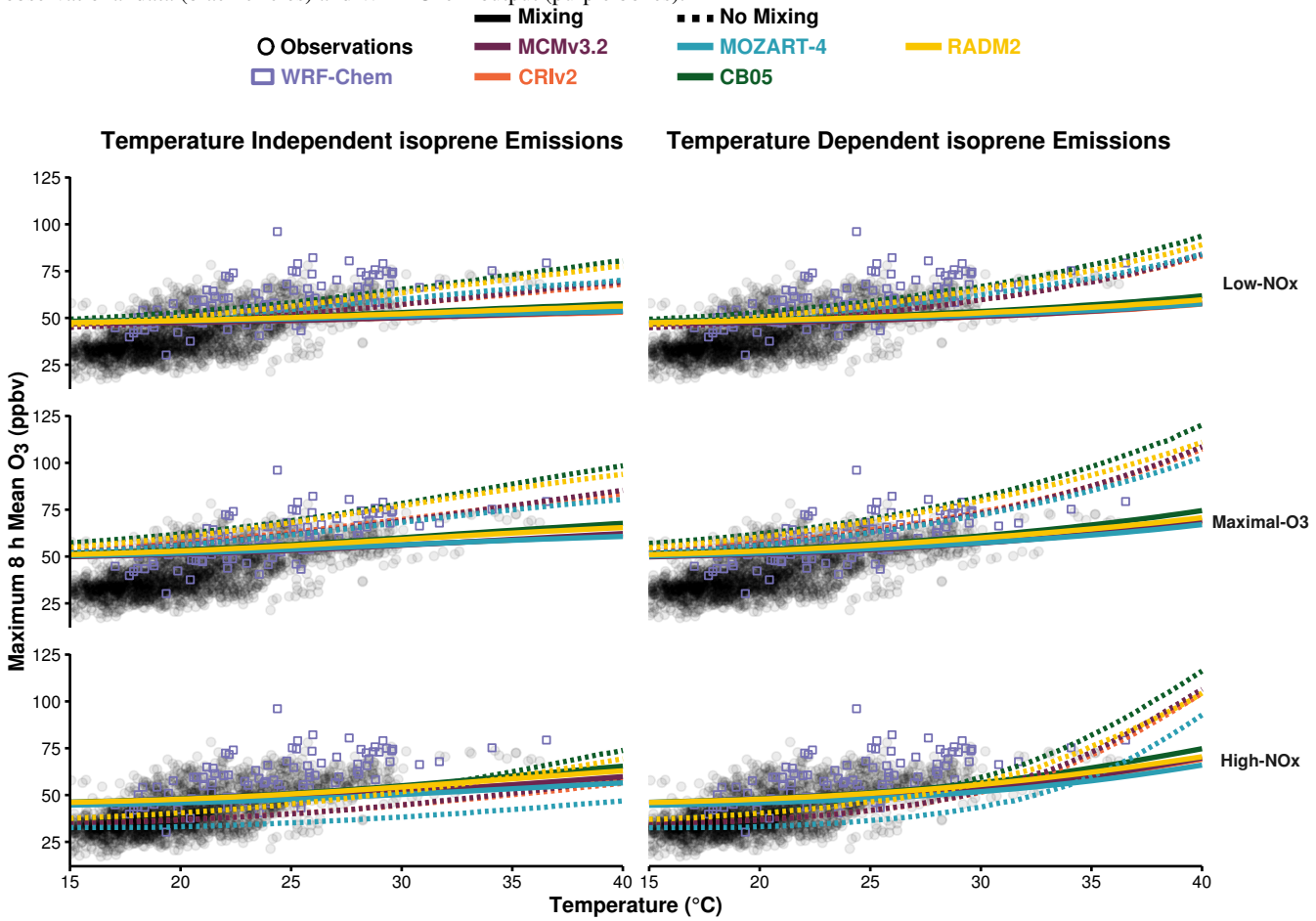

Table 3. Slopes ($m_{O3\text{-}T}$, ppbv per $^{\circ}$C) of the linear fit to MDA8 values of ozone and temperature correlations in Fig. 5, indicating the increase of MDA8 in ppbv of ozone per $^{\circ}$C. The slope of the observational data is 2.15 ppbv/$^{\circ}$C and the slope of the WRF-Chem output is 2.05 ppbv/$^{\circ}$C.

Mechanism	**Isoprene Emissions**	**Low-NO_x**		**Maximal-O_3**		**High-NO_x**	
		Mixing	**No Mixing**	**Mixing**	**No Mixing**	**Mixing**	**No Mixing**
MCMv3.2	Temperature Independent	0.28	1.01	0.51	1.36	0.59	0.96
	Temperature Dependent	0.42	1.48	0.74	2.16	0.93	2.63
CRIv2	Temperature Independent	0.25	0.93	0.47	1.27	0.55	0.88
	Temperature Dependent	0.40	1.44	0.71	2.09	0.90	2.52
MOZART-4	Temperature Independent	0.25	0.97	0.44	1.21	0.49	0.59
	Temperature Dependent	0.38	1.43	0.65	1.98	0.81	2.05
CB05	Temperature Independent	0.39	1.30	0.67	1.72	0.79	1.45
	Temperature Dependent	0.52	1.72	0.89	2.44	1.12	2.94
RADM2	Temperature Independent	0.37	1.31	0.61	1.64	0.70	1.28
	Temperature Dependent	0.48	1.68	0.79	2.22	0.97	2.49